JACS
JOURNAL OF THE AMERICAN CHEMICAL SOCIETY

Communication

pubs.acs.org/JACS

All-Polymer Solar Cells with 3.3% Efficiency Based on Naphthalene Diimide-Selenophene Copolymer Acceptor

Taeshik Earmme, Ye-Jin Hwang, Nishit M. Murari, Selvam Subramaniyan, and Samson A. Jenekhe*

Department of Chemical Engineering and Department of Chemistry, University of Washington, Seattle, Washington 98195-1750, United States

Supporting Information

ABSTRACT: The lack of suitable acceptor (n-type) polymers has limited the photocurrent and efficiency of polymer/polymer bulk heterojunction (BHJ) solar cells. Here, we report an evaluation of three naphthalene diimide (NDI) copolymers as electron acceptors in BHJ solar cells which finds that all-polymer solar cells based on an NDI-selenophene copolymer (PNDIS-HD) acceptor and a thiazolothiazole copolymer (PSEHTT) donor exhibit a record 3.3% power conversion efficiency. The observed short circuit current density of 7.78 mA/cm^2 and external quantum efficiency of 47% are also the best such photovoltaic parameters seen in all-polymer solar cells so far. This efficiency is comparable to the performance of similarly evaluated [6,6]-Phenyl-C_{61}-butyric acid methyl ester ($PC_{60}BM$)/PSEHTT devices. The lamellar crystalline morphology of PNDIS-HD, leading to balanced electron and hole transport in the polymer/polymer blend solar cells accounts for its good photovoltaic properties.

Solution-processed organic photovoltaic devices are promising low cost solar energy technologies.[1] Much progress has been made in developing polymer/fullerene solar cells in the past decade, with efficiencies now approaching 10%.[2] In contrast, the performance of all-polymer solar cells, composed of both *donor* and *acceptor* polymers and free of fullerenes, has remained relatively low with no significant advance in the same period.[3] All-polymer active layers of solar cells have potential advantages over polymer/fullerene systems, including enhanced absorption coefficients, increased photovoltage, superior photochemical, thermal, and mechanical robustness, and facile control of solution viscosity and the industrial coating process. Perylene diimide (PDI) and naphthalene diimide (NDI) have been the most widely explored building blocks[3,4] in the design and investigation of acceptor (n-type) polymers for all-polymer solar cells.[3,4] A PDI-based acceptor polymer in combination with polythiophene derivatives has produced bulk heterojunction (BHJ) solar cells with a power conversion efficiency (PCE) of 2.23%.[3h] An NDI-bithiophene copolymer (PNDI2OD-T2) with very high field-effect electron mobilities (0.1−0.85 cm^2/(V s)) and moderate bulk electron mobility (~10^{-3} cm^2/(V s)) has so far shown only low efficiencies of 0.2−1.4% PCE in BHJ solar cells using a P3HT donor polymer.[3e,l] Among the acceptor polymers in BHJ solar cells, a benzothiadiazole-fluorene copolymer has the highest PCE (2.7%) reported to date.[3k] The short circuit current density (J_{sc} < 6.3 mA/cm^2) and external quantum efficiency (EQE < 43%) obtained to date in all-polymer solar cells[3] have also been far lower than in polymer/fullerene devices.[1,2]

Here, we report all-polymer solar cells with 3.3% PCE enabled by a novel polymer/polymer blend system composed of a new NDI-selenophene copolymer acceptor and a thiazolothiazole-dithienosilole copolymer donor. Three n-type polymer semiconductors, including an NDI-thiophene copolymer (PNDIT) and two new NDI-selenophene copolymers (PNDIS, PNDIS-HD) whose molecular structures are shown in Figure 1a, are investigated as electron acceptors in BHJ solar cells for the first time. We show that these NDI-based copolymers exhibit *unipolar* electron transport with high field-effect and bulk mobilities. The donor polymer, poly[(4,4′-bis(2-ethylhexyl)dithieno[3,2-*b*:2′,3′-*d*]silole)- 2,6-diyl-*alt*-(2,5-bis(3-(2-ethylhexyl)thiophen-2-yl)thiazolo[5,4-*d*]thiazole)] (PSEHTT, Figure 1a) has been previously shown to be a promising electron donor and hole-conducting material in polymer/fullerene BHJ solar cells.[5] The morphology of the

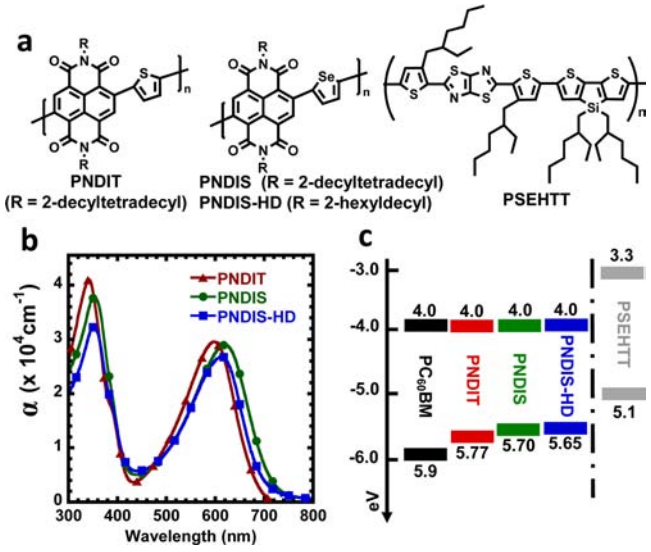

Figure 1. (a) Molecular structures of acceptor (PNDIT, PNDIS, and PNDIS-HD) and donor (PSEHTT) polymers. (b) UV−vis absorption spectra of PNDIT, PNDIS, and PNDIS-HD. (c) LUMO/HOMO energy levels of PNDIT, PNDIS, PNDIS-HD, $PC_{60}BM$, and PSEHTT.

Received: August 17, 2013
Published: October 1, 2013

   dx.doi.org/10.1021/ja4085429 | *J. Am. Chem. Soc.* 2013, 135, 14960−14963

Table 1. Molecular Weight, Thermal Stability, Photophysical, and XRD Properties of NDI-Copolymers

polymer	M_w (kDa)	M_n (kDa)	PDI	T_d (°C)	λ_{max}^{sol}	λ_{max}^{film}	E_g (eV)	d_{100} (Å)	d_{010} (Å)
PNDIT	31.5	23.9	1.3	430	326, 542	341, 598	1.77	24.86	4.20
PNDIS	31.6	26.1	1.2	415	341, 556	353, 621	1.70	22.92	4.16
PNDIS-HD	177.9	79.0	2.3	400	341, 556	351, 614	1.65	21.53	4.16

polymer/polymer blends was imaged by AFM. Charge transport in the active layer blends was investigated by organic field-effect transistors (OFETs) and space-charge-limited current (SCLC) measurements. Finally, we show that the all-polymer solar cells can be as efficient as the similarly evaluated $PC_{60}BM$/PSEHTT BHJ devices.

PNDIT and PNDIS were synthesized by Stille coupling copolymerization of 4,9-dibromo-2,7-bis(2-decyltetradecyl)-benzo[*lmn*][3,8]-phenanthroline-1,3,6,8-tetraone with 2,5-bis-(trimethylstannyl)thiophene and 2,5-bis(trimethylstannyl)-selenophene, respectively, in the presence of $Pd_2(dba)_3$ and P(*o*-tolyl)$_3$ in chlorobenzene solvent (Supporting Information (SI), Figure S1). PNDIS-HD was similarly synthesized as PNDIS using 4,9-dibromo-2,7-bis(2-hexyldecyl)benzo[*lmn*]-[3,8]-phenanthroline-1,3,6,8-tetraone with a shorter 2-hexyl-decyl (HD) side chain. The monomer and copolymer molecular structures were confirmed by ^{1}H NMR (SI, Figure S2–S7). The M_n of PNDIT and PNDIS was 23.9 and 26.1 kDa with a polydispersity index (PDI) of 1.3 and 1.2, respectively. PNDIS-HD had a much higher M_n of 79.0 kDa with a PDI of 2.3. These polymers had an onset decomposition temperature (T_d) of 400–430 °C (SI, Figure S8a).

X-ray diffraction (XRD) analysis of solution-cast films of PNDIT, PNDIS, and PNDIS-HD revealed lamellar crystallinity with an intense (100) peak (SI, Figure S8b). A lamellar *d*-spacing (d_{100}) of 24.86, 22.92, and 21.53 Å, respectively, was observed for PNDIT, PNDIS, and PNDIS-HD. The shorter d_{100} spacing compared to the alkyl chain length (2 × 14 C) of 43.12 Å indicates interdigitation of the alkyl chains. As expected, PNDIS-HD has a smaller d_{100} value compared to the other two polymers with 2-decyltetradecyl side chains. The shorter d_{100} spacing of PNDIS compared to PNDIT is due to a larger torsion angle between NDI and selenophene moieties, which is a consequence of the larger Se orbitals compared to S. The observed $\pi-\pi$ stacking distance (d_{010}) of 4.16 Å in PNDIS and PNDIS-HD and 4.2 Å in PNDIT are comparable with values seen in other NDI-based copolymers (~4.0 Å).[6]

Optical absorption spectra of PNDIT, PNDIS, and PNDIS-HD thin films (Figure 1b) and dilute (~10^{-6} M) $CHCl_3$ solutions (SI, Figure S8b) show two distinctive absorption peaks, one due to $\pi-\pi^*$ transition at 340–360 nm and the other centered at 598–621 nm, which is a result of intramolecular charge transfer (ICT) (Table 1). It is interesting that the selenophene-linked polymers, PNDIS and PNDIS-HD, have slightly smaller band gaps and a broader fwhm in the ICT bands, which imply potentially better near-IR light harvesting compared to the thiophene-linked PNDIT. At their visible absorption maxima of 598–621 nm, all three NDI copolymers have an absorption coefficient (α) of (2.7–2.9) × 10^4 cm^{-1}. In contrast, an absorption coefficient of 1.1 × 10^5 cm^{-1} is observed at the absorption maximum (584 nm) of the donor polymer (PSEHTT). The LUMO/HOMO energy levels of the NDI copolymers along with those of $PC_{60}BM$[7] and PSEHTT[5] are shown in Figure 1c. The LUMO energy levels of the NDI copolymers were estimated from cyclic voltammetry (SI, Figure S8c) while the corresponding HOMO energy levels were obtained from the LUMO levels and the optical band gaps.

The electron transport properties of PNDIT, PNDIS, and PNDIS-HD thin films were characterized by using organic field-effect transistors (OFETs) with bottom gate/top contact geometry. The OFETs showed only n-channel transistor behavior with unipolar electron transport. The average saturated region field-effect electron mobilities of PNDIT, PNDIS, and PNDIS-HD were 2 × 10^{-4}, 2 × 10^{-3}, and 7 × 10^{-3} $cm^2/(V\ s)$, respectively (SI, Figure S9). The order of magnitude higher electron mobility of PNDIS and PNDIS-HD compared to PNDIT can be understood from the larger π-orbitals of selenium compared to sulfur, which improves overlap of the orbitals. In addition, interaction between Se–Se atoms could enhance the crystallinity of the copolymers and interchain charge transport.[8] The higher electron mobility of PNDIS and PNDIS-HD can also be explained by their favorable solid state morphology and molecular packing with shorter d_{100} and d_{010} spacings compared to PNDIT (Table 1). The higher electron mobility of PNDIS-HD with shorter hexyldecyl side chains compared to PNDIS with decyltetradecyl side chains can be largely understood in terms of the higher molecular weight and shorter d_{100} spacing of PNDIS-HD.

We fabricated and evaluated polymer/polymer blend solar cells with the inverted device structure of ITO/ZnO/blend/MoO_3/Ag. The active layer blend was PNDIT:PSEHTT, PNDIS:PSEHTT, or PNDIS-HD:PSEHTT, each spin-coated from chlorobenzene with an optimum composition of 1:1 *w*/*w*. The optimal composition (1:1 *w*/*w*) to focus our detailed investigation was determined by the initial performance of solar cells fabricated from different blend compositions (1:0.75, 1:1, and 1:2 *w*/*w*). The photodiodes were fabricated in a glovebox and tested under AM 1.5 solar illumination at 100 mW/cm^2 in ambient conditions. Representative current density–voltage (*J*–*V*) curves of PNDIT:PSEHTT, PNDIS:PSEHTT, and PNDIS-HD:PSEHTT solar cells are shown in Figure 2a. The photovoltaic parameters including the short-circuit current density (J_{sc}), the open-circuit voltage (V_{oc}), and fill factor (*FF*) are summarized in Table 2.

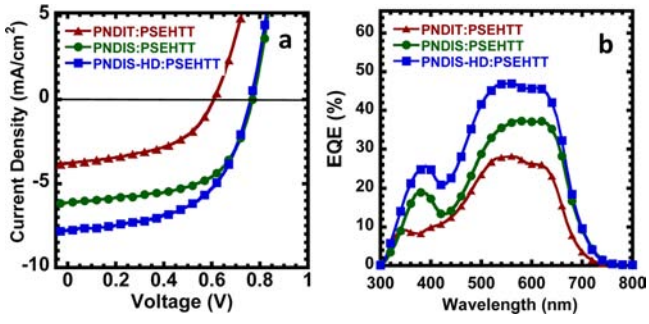

Figure 2. (a) Current density (*J*)–voltage (*V*) characteristics and (b) external quantum efficiency (EQE) spectra of all-polymer BHJ solar cells from 1:1 *w*/*w* blend each of PSEHTT:PNDIT, PSEHTT:PNDIS, and PSEHTT:PNDIS-HD.

dx.doi.org/10.1021/ja4085429 | J. Am. Chem. Soc. 2013, 135, 14960–14963

Table 2. Photovoltaic Properties of All-polymer Solar Cells

active layer (1:1 *w*/*w*)	J_{sc} (mA/cm^2)	V_{oc} (V)	FF	PCE_{avg} (%)	PCE_{max} (%)
PNDIT:PSEHTT	3.80	0.61	0.56	1.20 ± 0.09	1.30
PNDIS:PSEHTT	6.53	0.75	0.60	2.84 ± 0.15	2.96
PNDIS-HD:PSEHTT	7.78	0.76	0.55	3.16 ± 0.10	3.26

BHJ devices based on the thiophene-linked PNDIT acceptor showed the lowest performance among the three NDI copolymer acceptors, including a maximum 1.30% PCE and a rather low photocurrent (Table 2). The performance of the BHJ solar cells increased significantly by using the selenophene-linked PNDIS acceptor; the observed maximum PCE of 2.96% means a 2.4-fold increase compared with the PNDIT devices. This improvement arises from the higher J_{sc} of 6.53 mA/cm^2 as well as the increased V_{oc} of 0.75 V. The best performance, with a maximum PCE of 3.26%, J_{sc} = 7.78 mA/cm^2, and V_{oc} = 0.76 V, was observed in PNDIS-HD:PSEHTT blend solar cells, where the acceptor polymer has smaller hexyldecyl (HD) side chains. The lower photovoltage of PNDIT cells compared to those of PNDIS and PNDIS-HD is likely a result of greater charge recombination due to their much lower carrier mobilities. The observed *FF* values of 0.55−0.60 are impressively high among all-polymer solar cells and are comparable to typical values seen in polymer/fullerene systems. We note that both the PCE and photocurrent observed in PNDIS-HD devices are the highest for all-polymer solar cells reported to date.

The EQE spectra of the photovoltaic devices showed that the photocurrent generation starts at 720 nm (Figure 2b) and are consistent with the absorption spectra of the blends. The PNDIS-HD:PSEHTT device shows the highest photoconversion efficiency with a maximum EQE of 47% with more than 45% over the 500−650 nm wavelength range. The J_{sc} calculated by integrating the EQE spectrum of the PNDIS-HD:PSEHTT solar cell with an AM 1.5 reference spectrum is 7.76 mA/cm^2, which is in excellent agreement with the 7.78 mA/cm^2 measured directly from the *J*−*V* curve. We note that J_{sc} values calculated from the EQE spectra for the PNDIS and PNDIT devices were also within 3% of the J_{sc} values from *J*−*V* measurements. The maximum EQE seen in PNDIS-HD devices is the highest so far in all-polymer solar cells.

We also fabricated polymer/fullerene solar cells with the PSEHTT:$PC_{60}BM$ (1:2 *w*/*w*) active layer and the same inverted device structure as a reference for comparison with the polymer/polymer blend solar cells. In this case, we used the previously reported optimized composition and processing conditions to deposit the PSEHTT:$PC_{60}BM$ active layer, including the 3.0 vol % 1,8-diiodooctane (DIO) additive in *o*-dichlorobenzene.[5b] From the *J*−*V* characteristics (SI, Figure S11a) we obtained J_{sc} = 8.46 mA/cm^2, V_{oc} = 0.64 V, *FF* = 0.62, and a maximum PCE of 3.3% (average PCE 3.23 ± 0.11). This performance is in good agreement with the previous report.[5b] The EQE spectrum of the optimum PSEHTT:$PC_{60}BM$ cell shows the same onset of photocurrent as the above all-polymer devices; however, the 54% maximum EQE (SI, Figure S11b) is higher than the 47% observed for the all-polymer BHJ solar cells. Although the EQE and the photocurrent of $PC_{60}BM$ devices are higher than those of the polymer acceptor, PNDIS-HD, the power conversion efficiencies of BHJ solar cells using the two types of acceptors are identical largely because of the superior photovoltage of the all-polymer devices.

The charge transport properties of the polymer/polymer blends (PSEHTT:PNDIT, PSEHTT:PNDIS, and PSEHTT:PNDIS-HD) in the all-polymer solar cells were investigated by both OFET devices and space-charge-limited current (SCLC) measurements and are summarized in Table 3. Field-effect electron mobility in PNDIS-HD blends (1.3×10^{-4} cm^2/(V s)) was slightly better than in PNDIS blends but an order of magnitude higher than in PNDIT blends. In contrast, the field-effect hole mobility was about the same in all three series of blends (3.5−6.4) × 10^{-4} cm^2 /(V s). Hole-only devices, composed of ITO/PEDOT:PSS/blend/Au, and electron-only devices, consisting of ITO/ZnO/blend/LiF/Al, enabled estimation of the bulk charge transport properties of the BHJ blend films. Electron mobility in the bulk blend film is also highest in the PNDIS-HD blends (1.0×10^{-4} cm^2/(V s)), slightly lower in PNDIS blends (5.8×10^{-5} cm^2/(V s)), and a factor of 6 lower in the PNDIT blends (1.8×10^{-5} cm^2/(V s)). Balanced and high hole and electron mobilities are thus observed in the PNDIS-HD blends (Table 3), which can largely explain the highest performance in terms of J_{sc}, EQE, and PCE values for the BHJ solar cells using this polymer acceptor.

AFM imaging was used to investigate the surface morphology of the all-polymer solar cells. AFM topographic and the corresponding phase images taken directly from the surfaces of devices are shown in Figure 3. The observed phase separated morphology with domain sizes of 200−500 nm is identical in all three blend systems (PNDIT, PNDIS, and PNDIS-HD). The similarity of the morphology of all three different polymer/polymer BHJ devices implies that the observed large variation in the photocurrent and PCE does not originate in the blend morphologies. On the other hand, the large scale of the observed phase separation in the blends suggests that there is still room for further improvement of the photovoltaic properties of PNDIS:PSEHTT and PNDIS-HD:PSEHTT blends by reducing the domain sizes of the phase separated blend morphology through strategies such as cosolvents[3e,h] and processing additives.[9]

In conclusion, two new semicrystalline NDI copolymers (PNDIS, PNDIS-HD) and a known one (PNDIT) have been synthesized, characterized, and, for the first time, evaluated as acceptors in BHJ organic solar cells. We found that all-polymer solar cells composed of a PNDIS-HD acceptor and PSEHTT

Table 3. Charge Transport Properties of Polymer/Polymer Blends Used in All-Polymer Solar Cells

blend (1:1 *w*/*w*)	μ_h[a] (cm^2/(V s)) (OFET)	μ_e[b] (cm^2/(V s)) (OFET)	μ_h[c] (cm^2/(V s)) (SCLC)	μ_e[d] (cm^2/(V s)) (SCLC)
PNDIT:PSEHTT	4.0×10^{-4}	1.0×10^{-5}	4.5×10^{-5}	1.8×10^{-5}
PNDIS:PSEHTT	3.5×10^{-4}	7.5×10^{-5}	9.6×10^{-5}	5.8×10^{-5}
PNDIS-HD:PSEHTT	6.4×10^{-4}	1.3×10^{-4}	2.0×10^{-4}	1.0×10^{-4}

[a]Average charge carrier mobility of blend from p-channel OFETs. [b]Average charge carrier mobility of blend from n-channel OFETs. [c]Hole mobility of blend extracted from SCLC measurement using single charge carrier devices. [d]Electron mobility of blend extracted from SCLC measurement using single charge carrier devices.

dx.doi.org/10.1021/ja4085429 | J. Am. Chem. Soc. 2013, 135, 14960−14963

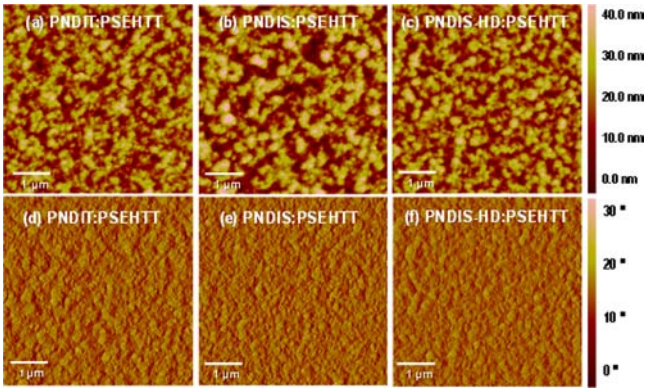

Figure 3. AFM topographical images (5 × 5 μm^2) of the surfaces of all-polymer solar cells: (a) PNDIT:PSEHTT, (b) PNDIS:PSEHTT, and (c) PNDIS-HD:PSEHTT; and the corresponding phase images of (d) PNDIT:PSEHTT, (e) PNDIS:PSEHTT, and (f) PNDIS-HD:PSEHTT.

donor have a record performance (PCE = 3.3%, J_{sc} = 7.78 mA/cm^2, and EQE = 47%), which is comparable to similarly evaluated $PC_{60}BM$:PSEHTT BHJ solar cells. Balanced electron and hole transport was observed in the PNDIS-HD:PSEHTT blend active layers. The superior photovoltaic properties of PNDIS-HD compared to PNDIS and prior NDI copolymers[3e,n] suggest that unipolar electron transport with high bulk mobility, good crystallinity, size of alkyl side chains, and molecular weight are all important factors in the design of suitable acceptor polymers for BHJ solar cells.

■ ASSOCIATED CONTENT

Supporting Information

Experimental procedures, NMR spectra, TGA thermograms, UV−vis absorption spectra, cyclic voltammograms (CV), and XRD patterns of copolymers, OFETs, PSEHTT:$PC_{60}BM$ solar cell, and SCLC device characteristics. This material is available free of charge via the Internet at http://pubs.acs.org.

■ AUTHOR INFORMATION

Corresponding Author

jenekhe@u.washington.edu

Notes

The authors declare no competing financial interest.

■ ACKNOWLEDGMENTS

This paper is based on work (Excitonic Solar Cells) supported by the U.S. Department of Energy, Office of Basic Energy Sciences, Division of Materials Sciences, under Award DEFG02-07ER46467. The synthesis, characterization, and charge transport properties of the n-type copolymers were supported by the Office of Naval Research (ONR) (N00014-11-1-0317) and the NSF (DMR-1035196).

■ REFERENCES

(1) (a) Günes, S.; Neugebauer, H.; Sariciftci, N. S. *Chem. Rev.* **2007**, *107*, 1324. (b) Thompson, B. C.; Fréchet, J. M. J. *Angew. Chem., Int. Ed.* **2008**, *47*, 58. (c) Li, G.; Zhu, R.; Yang, Y. *Nat. Photon.* **2012**, *6*, 153.

(2) (a) You, J.; Dou, L.; Yoshimura, K.; Kato, T.; Ohya, K.; Moriarty, T.; Emery, K.; Chen, C.-C.; Gao, J.; Li, G.; Yang, Y. *Nat. Commun.* **2013**, *4*, 1446. (b) He, Z.; Zhong, C.; Su, S.; Xu, M.; Wu, H.; Cao, Y. *Nat. Photon.* **2012**, *6*, 591. (c) Small, C. E.; Chen, S.; Subbiah, J.; Amb, C. M.; Tsang, S.-W.; Lai, T.-H.; Reynolds, J. R.; So, F. *Nat. Photon.* **2012**, *6*, 115.

(3) (a) McNeill, C. R. *Energy Environ. Sci.* **2012**, *5*, 5653. (b) Facchetti, A. *Mater. Today* **2013**, *16*, 123. (c) Halls, J. J. M.; Walsh, C. A.; Greenham, N. C.; Marseglia, E. A.; Friend, R. H.; Moratti, S. C.; Holmes, A. B. *Nature* **1995**, *376*, 498. (d) Alam, M. M.; Jenekhe, S. A. *Chem. Mater.* **2004**, *16*, 4647. (e) Schubert, M.; Dolfen, D.; Frisch, J.; Roland, S.; Steyrleuthner, R.; Stiller, B.; Chen, Z.; Scherf, U.; Koch, N.; Facchetti, A.; Neher, D. *Adv. Energy Mater.* **2012**, *2*, 369. (f) Jenekhe, S. A.; Yi, S. *Appl. Phys. Lett.* **2000**, *77*, 2635. (g) Zhou, E.; Tajima, K.; Yang, C.; Hashimoto, K. *J. Mater. Chem.* **2010**, *20*, 2362. (h) Zhou, E.; Cong, J.; Wei, Q.; Tajima, K.; Yang, C.; Hashimoto, K. *Angew. Chem., Int. Ed.* **2011**, *50*, 2799. (i) Kietzke, T.; Hörhold, H.-H.; Neher, D. *Chem. Mater.* **2005**, *17*, 6532. (j) Holcombe, T. W.; Woo, C. H.; Kavulak, D. F. J.; Thompson, B. C.; Fréchet, J. M. J. *J. Am. Chem. Soc.* **2009**, *131*, 14160. (k) Mori, D.; Benten, H.; Ohkita, H.; Ito, S.; Miyake, K. *ACS Appl. Mater. Interfaces* **2012**, *4*, 3325. (l) Zhan, X.; Tan, Z. a.; Domercq, B.; An, Z.; Zhang, X.; Barlow, S.; Li, Y.; Zhu, D.; Kippelen, B.; Marder, S. R. *J. Am. Chem. Soc.* **2007**, *129*, 7246. (m) Zhou, E.; Cong, J.; Zhao, M.; Zhang, L.; Hashimoto, K.; Tajima, K. *Chem. Commun.* **2012**, *48*, 5283. (n) Hwang, Y.-J.; Ren, G.; Murari, N. M.; Jenekhe, S. A. *Macromolecules* **2012**, *45*, 9056. (o) Cao, Y.; Lei, T.; Yuan, J.; Wang, J.-Y.; Pei, J. *Polym. Chem* **2013**, *4*, 5228. (p) Moore, J. R.; Albert-Seifried, S.; Rao, A.; Massip, S.; Watts, B.; Morgan, D. J.; Friend, R. H.; McNeill, C. R.; Sirringhaus, H. *Adv. Energy Mater.* **2011**, *1*, 230. (q) Brenner, T. J. K.; Hwang, I.; Greenham, N. C.; McNeill, C. R. *J. Appl. Phys.* **2010**, *107*, 114501. (r) Guo, C.; Lin, Y.-H.; Witman, M. D.; Smith, K. A.; Wang, C.; Hexemer, A.; Strzalka, J.; Gomez, E. D.; Verduzco, R. *Nano Lett.* **2013**, *13*, 2957.

(4) (a) Anthony, J. E.; Facchetti, A.; Heeney, M.; Marder, S. R.; Zhan, X. *Adv. Mater.* **2010**, *22*, 3876. (b) Mishra, A.; Bäuerle, P. *Angew. Chem., Int. Ed.* **2012**, *51*, 2020.

(5) (a) Subramaniyan, S.; Xin, H.; Kim, F. S.; Shoaee, S.; Durrant, J. R.; Jenekhe, S. A. *Adv. Energy Mater.* **2011**, *1*, 854. (b) Xin, H.; Subramaniyan, S.; Kwon, T.-W.; Shoaee, S.; Durrant, J. R.; Jenekhe, S. A. *Chem. Mater.* **2012**, *24*, 1995.

(6) (a) Hwang, Y.-J.; Murari, N. M.; Jenekhe, S. A. *Polym. Chem.* **2013**, *4*, 3187. (b) Guo, X.; Kim, F. S.; Seger, M. J.; Jenekhe, S. A.; Watson, M. D. *Chem. Mater.* **2012**, *24*, 1434.

(7) Scharber, M. C.; Mühlbacher, D.; Koppe, M.; Denk, P.; Waldauf, C.; Heeger, A. J.; Brabec, C. J. *Adv. Mater.* **2006**, *18*, 789.

(8) (a) Chen, Z.; Lemke, H.; Albert-Seifried, S.; Caironi, M.; Nielsen, M. M.; Heeney, M.; Zhang, W.; McCulloch, I.; Sirringhaus, H. *Adv. Mater.* **2010**, *22*, 2371. (b) Hollinger, J.; Jahnke, A. A.; Coombs, N.; Seferos, D. S. *J. Am. Chem. Soc.* **2010**, *132*, 8546.

(9) Ren, G.; Ahmed, E.; Jenekhe, S. A. *Adv. Energy Mater.* **2011**, *1*, 946.